Thermodynamic and Structure Guided Design of Statin Based Inhibitors of 3-Hydroxy-3-Methylglutaryl Coenzyme A Reductase

Ronald W. Sarver,*[,†] Elizabeth Bills,[‡] Gary Bolton,[§] Larry D. Bratton,[||] Nicole L. Caspers,[⊥] James B. Dunbar,[#] Melissa S. Harris,[▽] Richard H. Hutchings,[○] Robert M. Kennedy,[#] Scott D. Larsen,[#] Alexander Pavlovsky,[◆] Jeffrey A. Pfefferkorn,[¶] and Graeme Bainbridge[+]

Pfizer Global Research & Development, Ann Arbor, Michigan 48105

Received December 3, 2007

Clinical studies have demonstrated that statins, 3-hydroxy-3-methylglutaryl coenzyme A reductase (HMGR) inhibitors, are effective at lowering mortality levels associated with cardiovascular disease; however, 2–7% of patients may experience statin-induced myalgia that limits compliance with a treatment regimen. High resolution crystal structures, thermodynamic binding parameters, and biochemical data were used to design statin inhibitors with improved HMGR affinity and therapeutic index relative to statin-induced myalgia. These studies facilitated the identification of imidazole **1** as a potent ($IC_{50} = 7.9$ nM) inhibitor with excellent hepatoselectivity (>1000-fold) and good in vivo efficacy. The binding of **1** to HMGR was found to be enthalpically driven with a ΔH of –17.7 kcal/M. Additionally, a second novel series of bicyclic pyrrole-based inhibitors was identified that induced order in a protein flap of HMGR. Similar ordering was detected in a substrate complex, but has not been reported in previous statin inhibitor complexes with HMGR.

Introduction

Although progress has been made at reducing the number of deaths in the United States due to cardiovascular disease, statistics from the American Heart Association indicate that cardiovascular diseases are still the major cause of death, responsible for about 36% of deaths in the United States in 2004.[1] This study also indicated that, in addition to age, major factors for increased risk of cardiovascular diseases were stage 2 hypertension, hypercholesterolemia (>240 mg/dL), smoking, and diabetes. In addition to diet and exercise, there are treatment options available to reduce these risk factors. Statins, a class of compounds known to inhibit 3-hydroxy-3-methylglutaryl coenzyme A (HMG-CoA)[a] reductase, have been proven clinically effective at lowering circulating low density lipoprotein cholesterol (LDL-c) levels and reducing cardiovascular disease.[2–5] There is also evidence that additional clinical benefit may be obtained from some statins through mechanisms unrelated to HMG-CoA reductase inhibition.[6] While most statins are well tolerated and have good safety profiles, a small number of patients have experienced myalgia related to the effect of statins on muscle tissue.[7–9] While the overall incidence of myalgia is low (2–7% of patients in clinical trials), the likelihood of occurrence increases with drug dose and it can be a key factor in preventing patient compliance with a treatment regimen. Physiologically, the mechanism of statin-induced myalgia is complex but thought to involve, in part, inhibition of HMG-CoA reductase in nonhepatic tissues (particularly muscle) thereby disrupting the biosynthesis of isoprenoid-derived biomolecules important in post-translational protein modification (i.e., prenylation) and electron transport (i.e., ubiquinone). There is evidence that the likelihood of statin-induced myalgia can be reduced by targeting HMG-CoA reductase inhibitors to hepatic tissues and limiting peripheral exposure, and it has been demonstrated that the hepatoselectivity of a given HMG-CoA reductase inhibitor is related to its degree of lipophilicity.[10–13] In general, lipophilic statins tend to achieve higher levels of exposure in nonhepatic peripheral tissues, whereas more hydrophilic statins tend to be more hepatoselective.[9,14]

To meet the challenge of finding novel HMG-CoA reductase inhibitors with improved efficacy and tolerability, we undertook a discovery effort to identify a novel series of inhibitors with best-in-class preclinical efficacy and hepatoselectivity. Hepatoselectivity was modulated by controlling inhibitor lipophilicity, while enzyme inhibition potency was optimized through structure–activity studies supported by ITC, which was utilized to understand the binding thermodynamics of structurally diverse inhibitors. Because entropically driven ligand−protein binding is typically associated with hydrophobic interactions whereas enthalpically driven binding is driven through electrostatic and H-bonding interactions, we favored templates with greater enthalpic components to their binding interactions as a way to minimize inhibitor lipophilicity, thereby increasing hepatoselectivity.

In mammals, the tetrameric HMGR enzyme is involved in cholesterol production through what is referred to as the

* Corresponding author. Phone: 860-686-9290. E-mail: Ronald.w.sarver@pfizer.com. Address: Ronald W. Sarver, Pfizer Global Research & Development, B118W-104, Eastern Point Road, Groton, Connecticut 06340.

[†] Current Address: Protein Cell and Assay Technologies, Pfizer Inc., Groton, Connecticut.

[‡] Current Address: Inhalation and Devices, Pfizer Inc., Sandwich, United Kingdom.

[§] Current Address: AAPharmaSyn LLC, Ann Arbor, Michigan.

[||] Current Address: Cayman Chemical Co., Ann Arbor, Michigan.

[⊥] Current Address: Structure and Computational Chemistry, Pfizer Inc., St. Louis, Missouri.

[#] Current Address: University of Michigan, Ann Arbor, Michigan.

[▽] Current Address: Structural Biology, Pfizer Inc., Groton, Connecticut.

[○] Current Address: Biogen Idec, Cambridge, Massachusetts.

[◆] Current Address: University of Toledo, Toledo, Ohio.

[¶] Current Address: Cardiovascular and Metabolic Diseases Chemistry, Pfizer Inc., Groton, Connecticut.

[+] Current Address: Protein Therapeutics, Pfizer Inc., St. Louis, Missouri.

[a] Abbreviations: Co-A, coenzyme A; DHHA, 3,5-dihyroxyheptanoic acid; GAP-pyruvate, glyceraldehyde-3-phosphate-pyruvate; HMGR, 3-hydroxy-3-methylglutaryl coenzyme A reductase; MAICS, mouse acute inhibition of cholesterol synthesis; ITC, isothermal titration calorimetry; LDL-c, low density lipoprotein cholesterol; TCEP, tris (2-carboxyethyl)phosphine; EDTA, ethylenediamine-tetraacidic acid; NADPH, β-nicotinamide adenine dinucleotide phosphate; PEG, polyethylene glycol; DTT, dithiothreitol.

10.1021/jm7015057 CCC: $40.75
Published on Web 06/10/2008

mevalonate pathway of isoprenoid production. Depending on species, isoprenoids are enzymatically synthesized through either the mevalonate pathway or the glyceraldehyde-3-phosphate-pyruvate (GAP-pyruvate) pathway, also known as the nonmevalonate pathway. Isoprenoids are involved in many cellular processes critical to cell growth and metabolism, but excess cholesterol production increases risk for cardiovascular disease. This and the importance of isoprenoids in cell function have made several enzymes involved in their synthesis important targets for regulation both in mammals and bacteria. High resolution crystal structures of inhibitors bound to the catalytic portion of HMGR and enzymatic studies have provided mechanistic details on HMGR inhibition.[15–19] Previous studies have indicated that statins are competitive inhibitors of substrate HMG-CoA but not competitive with NADPH.[16,20] Recently, thermodynamic information has provided information on the driving forces for HMGR inhibition by several statins.[21] In the present work, biochemical assays, microcalorimetry, and crystallography were conducted in parallel to determine the structural and thermodynamic parameters contributing to inhibitor binding interactions with HMGR. This information was used to improve inhibitor affinity and therapeutic window with respect to myalgia. In addition, thermodynamic parameters of substrate interaction with HMGR and substrate competition of statin inhibitors with HMGR were examined.

Results and Discussion

While several currently marketed statins are effective at lowering serum low density lipoprotein concentrations, some are much more effective at lowering LDL-c and also differ in their potential for adverse side-effects. To further increase potency and lower the potential for adverse side-effects, a concerted effort was undertaken to identify statins with increased HMGR affinity and preferential penetration into hepatic relative to muscle tissues. Hepatoselectivity was influenced by modulating inhibitor lipophilicity. Starting with several structurally diverse templates, compounds were synthesized and binding affinity to HMGR was determined using ITC. All analogues were evaluated for inhibitory potency in a HMG-CoA reductase enzyme inhibition assay.[22,23] Additionally, the ability of analogues to block cholesterol synthesis in both rat hepatocyte and myocyte cell lines was evaluated; moreover, comparison of these two values was utilized as a measurement of hepatoselectivity.[22,23] Table 1 shows the molecular structure, biological activity, and ITC results for the binding interaction of inhibitors with HMGR at 30 °C for a set of structurally diverse inhibitors clustered into six template subtypes (in addition to the substrate HMG-CoA and benchmark rosuvastatin). A high resolution costructure for each of the inhibitors in Table 1 was also solved with HMGR and representative structures from each class deposited in the Protein Data Bank. Inhibitors in series 1 and 2 contain a core imidazole heterocycle and vary in positioning of the substituents. For series 1, the imidazole nitrogen at the 1-position has a chiral 3,5-dihyroxyheptanoic acid (DHHA) substituent that mimics 3-hydroxy-3-methylglutaryl acid, while series 2 has an isopropyl at the 1-position and a DHHA moiety at the 2-position. Inhibitors in series 3 are bicyclic, containing a core pyrrole heterocycle. Series 4 inhibitors also have a core pyrrole heterocycle but are close analogues of atorvastatin with the DHHA substituent at the 1-position. Series 5 inhibitors are isomers of atorvastatin containing a core pyrrole heterocycle with the DHHA substituent at the 2-position. Series 6 inhibitors have a central pyrrole with the DHHA moiety at the 1-position but have a sulfonamide substituent at the 4-position of the pyrrole.

HMG-CoA and Rosuvastatin Binding to HMGR. Prior to examining inhibitor binding to HMGR, the binding of HMG-CoA was examined by ITC. Figure 1 shows the binding isotherm obtained for the interaction of 0.36 mM HMG-CoA with 0.020 mM HMGR at 30 °C. The stoichiometry for the interaction was approximately 1 molecule of HMG-CoA bound per HMGR. Other thermodynamic parameters obtained for the interaction were, ΔH of −9.0 kcal/M, and K_a of 6.9×10^4 M^{-1} or in terms of equilibrium dissociation constant, K_d, 1.4 μM ($K_d = 1/K_a$). Interaction of statins with apo HMGR were then investigated by ITC.

The binding interaction of rosuvastatin, **26**, to HMGR was examined by ITC, and the measured binding enthalpy was −13.2 kcal/M at 30 °C. Extrapolating to 37 °C using the change in heat capacity of −0.46 kcal/K^{-1} M^{-1}, as previously reported,[21] resulted in a ΔH of −16.4 kcal/M, in excellent agreement with that reported by Holdgate[24] of −16.6 kcal/M.

Although the trend of lower binding enthalpy compared to rosuvastatin was still apparent, measured binding enthalpies of –11.7 and −10.3 kcal/M at 30 °C for **13** and **14**, close analogues of atorvastatin, were ∼2 fold greater than that reported for atorvastatin by Carbonell et.al.[21] adjusted to 30 °C. The difference in binding enthalpy could be due to structural differences. Lafont et.al. showed for an HIV-1 protease inhibitor that replacing a thioether group with a sulfonyl resulted in a hydrogen bond that increased the binding enthalpy by 3.9 kcal/M.[25] With current microcalorimeter sensitivity limits, aqueous compound solubility for hydrophobic compounds can also be problematic for collection of ITC data. Although compound concentration is determined prior to ITC, usually kinetic solubility not thermodynamic solubility is determined. Data provided in Table 1 represent the average of two or more ITC experiments and only those data where binding enthalpy variability was less than 0.5 kcal/M were reported. This would help to eliminate inclusion of data for compounds where kinetic solubility was poor.

Inhibitors **1**–**5** and **7** and **8** with the core imidazole heterocycle had greater binding enthalpies than rosuvastatin and also better binding enthalpies than **13** and **14**, the atorvastatin analogues. Greater binding enthalpy is generally a very favorable feature for template selection.[21,25] Nonspecific binding is associated more with the hydrophobic effect, which is an entropy driven process. Compounds with enthalpically driven binding usually have significant H-bonding and electrostatic interactions that contribute to binding free energy resulting in greater binding specificity. In addition, compounds with large enthalpic binding components can afford to sacrifice some binding enthalpy to gain binding entropy. Binding entropy can be gained by adding hydrophobic substituents with complementary shape to the binding pocket producing an overall gain in binding free energy. Carbonell, et al. also showed that for a small set of statins where the conformation of HMGR did not change significantly, there was a correlation of binding enthalpy to binding affinity.

Detailed Thermodynamic Parameters for Imidazole Inhibitor 1 Binding to HMGR. Because binding enthalpy was more favorable for the imidazole series and for compound **1** in particular, additional calorimetry was performed to better characterize the binding interaction of **1** with HMGR. Shown in Figure 2a is the interaction of inhibitor **1** with HMGR as determined by ITC at 28 °C. In Figure 2a, mole ratio is expressed relative to monomeric HMGR and stoichiometry for the interaction was 1.1 mol of 1 per mole of HMGR. Im-

Table 1. Thermodynamic Parameters for the Binding Interactions of Inhibitors with HMGR Determined by ITC at 30°C and Inhibition of Cholesterol Synthesis in Rat Liver Microsomes, Rat Hepatocytes, L6 Myocytes, and Mouse Acute Inhibition of Cholesterol Synthesis

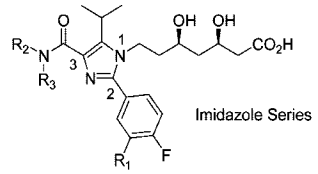

cmpd	R1	R2	R3	K_d (nM)	ΔG (kcal/M)	ΔH (kcal/M)	- TΔS (kcal/M)	RM IC_{50}[a] (nM)	HEP IC_{50}[a] (nM)	L6 IC_{50}[a] (nM)	L6/HEP	MAICS (%)	clogD (pH 7.4)
HMG-CoA				14450.9	-6.7	-9.1	2.4						
1	H	benzyl	H	13.5	-10.9	-17.7	6.7	7.9	0.30	3030	10100	-45	-0.84
2	F	benzyl	H	6.9	-11.3	-15.9	4.6	0.3	0.15	484	3227		-0.7
3	H	4-Ph-benzyl	H	9.7	-11.1	-15.2	4.1	3.6	0.47			-25	0.92
4	H	(*S*)-CH(CH_2OH)Ph	H	51.7	-10.1	-14.6	4.5	1.1	1.03	53700	52136	-18	-1.36
5	H	(S)-CH(CH_3)Ph	Me	7.5	-11.3	-14.1	2.9	1.9	0.17	23400	140120	-60	-1.23
6	H	3-(2-F-Ph)-benzyl	H	22.0	-10.6	-8.9	-1.7	0.6	13.90	617	44		1.42

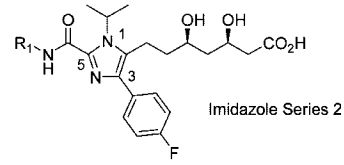

7	3-F-benzyl			26.9	-10.5	-17.7	7.2	2.9	0.99	84	85	-49	-0.7
8	benzyl			31.6	-10.4	-16.4	6.0	3.6	0.38	101	264	-74	-0.75

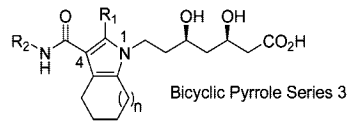

cmpd	R1	R2	n (# carbon atoms)	K_d (nM)	ΔG (kcal/M)	ΔH (kcal/M)	- TΔS (kcal/M)	RM IC_{50}[a] (nM)	HEP IC_{50}[a] (nM)	L6 IC_{50}[a] (nM)	L6/HEP	MAICS (%)	clogD (pH 7.4)
9	Et	4-Ph-benzyl	2	12.7	-10.9	-8.3	-2.7	5.1	1.16			11	2.15
10	*i*Pr	(*S*)-CH(CH_2OH)Ph	1	34.8	-10.3	-7.6	-2.7	7.8	2.34			-26	-0.32
11	*i*Pr	-benzyl	2	62.5	-10.0	-6.9	-3.1	3.6	26.40			-37	0.76
12	Et	4-Ph-benzyl	1	40.7	-10.2	-5.2	-5.1	11.5	0.68	1010	1487	-23	1.59

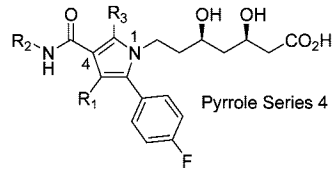

cmpd	R1	R2	R3	K_d (nM)	ΔG (kcal/M)	ΔH (kcal/M)	- TΔS (kcal/M)	RM IC_{50}[a] (nM)	HEP IC_{50}[a] (nM)	L6 IC_{50}[a] (nM)	L6/HEP	MAICS (%)	clogD (pH 7.4)
13	Ph	(2-OH)-Ph	*i*Pr	27.4	-10.5	-11.7	1.2						1.03
14	*i*Pr	Ph	Et	68.5	-9.9	-10.3	0.4	1.8	1.34			-50	1.02

Table 1. (Continued)

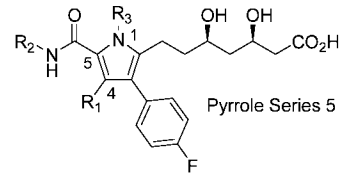

cmpd	R1	R2	R3	K_d (nM)	ΔG (kcal/M)	ΔH (kcal/M)	- TΔS (kcal/M)	RM IC_{50}[a] (nM)	HEP IC_{50}[a] (nM)	L6 IC_{50}[a] (nM)	L6/HEP	MAICS (%)	clogD (pH 7.4)
15	Ph	4-(SO_2NH_2)-Ph	CH3	26.3	-10.5	-13.7	3.1	3.0	0.27	1790	6704	-32	-0.88
16	Me	Ph	H	6.2	-11.4	-13.5	2.1	2.8	0.29			-53	-0.65
17	4-F-Ph	4-($CONMe_2$)-Ph	CH3	5.4	-11.5	-13.1	1.6	1.7	3.63	985	271	-59	-1.19
18	Ph	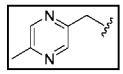	CH3	14.0	-10.9	-12.2	1.3	2.2	0.31	4650	15147	-36	-0.27
19	Ph	4-(CO_2Me)-Ph	CH3	9.4	-11.1	-12.0	0.9	0.5	0.12	57.3	478	-64	0.64
20	4-F-Ph	Ph	CH3	14.3	-10.9	-11.4	0.5	1.8	1.03			-57	0.16
21	4-F-Ph	3-Me-Ph	CH3	3.2	-11.8	-10.9	-0.9	1.3	2.81			-30	0.62
		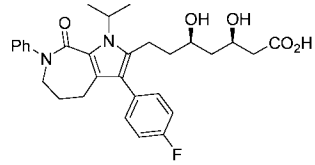											
22				21.6	-10.6	-7.9	-2.7	0.3	5.89			-39	-0.27
		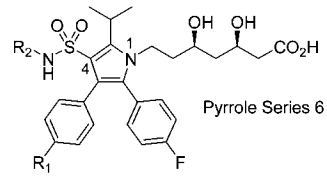											
23	F	4-(CO_2Me)-Ph		95.7	-9.7	-13.5	3.7	5.82	1.8			-34	-0.04
24	H	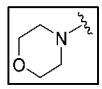		21.3	-10.6	-13.2	2.5	4.54	0.802	10000	12469	-56	-0.23
25	F	4-(CH_2CO_2Me)-Ph		42.7	-10.2	-13.0	2.8	1.04	1.37	10000	7299		-0.57
		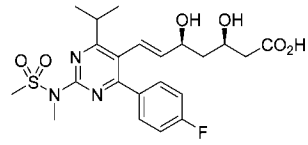											
26				17.0	-10.8	-13.2	2.4	3.6	0.23	720	3130	-82	-2.71

[a] RM, HEP, and L6 are inhibition of cholesterol synthesis of rat microsomal HMG-CoA reductase, in rat liver hepatocytes, and in rat muscle myocytes, respectively; L6/HEP, ratio of muscle myocyte to liver hepatocyte inhibition; MAICS, mouse acute inhibition of cholesterol synthesis. All compounds were tested at a dose of 30 mg/kg in the MAICS assay.

mediately apparent, based on the steep slope of the binding curve, was the much tighter binding affinity of **1** for HMGR than detected for HMG-CoA binding to HMGR. In addition, the interaction of **1** with HMGR had a large binding enthalpy relative to currently marketed statins where thermodynamic data were available.[21] Thermodynamic parameters for binding of **1** to HMGR at 28 °C were $N = 1.1$, ΔH of -14.1 ± 0.4 kcal/M, and a K_d of 29 nM. For accurate K_d determinations, recommended C values are between 1 and 1000. The value of C is calculated based on the product of the affinity of the ligand

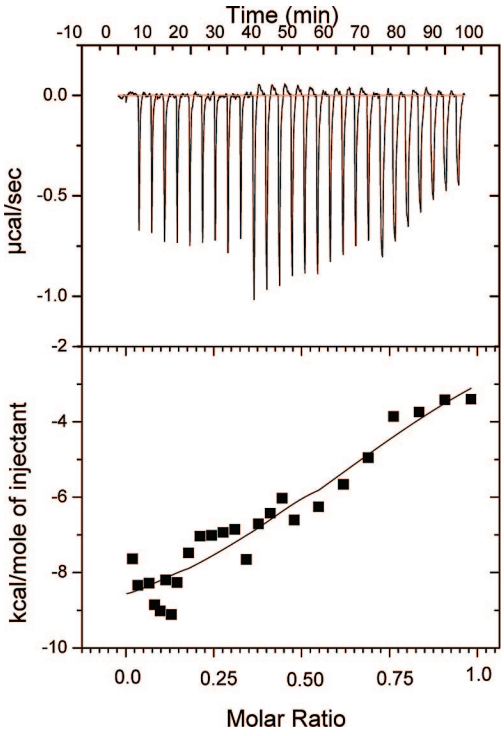

Figure 1. Binding isotherm obtained by ITC using one 1 μL, ten 4 μL, ten 8 μL, and ten 20 μL injections of 360 μM HMG-CoA into 20 μM HMGR at 28 °C in 10 mM Hepes, pH 7.2, 10% glycerol, 1 mM EDTA, 150 mM NaCl, 1.0 mM TCEP.

and the concentration of enzyme.[26] For inhibitor **1** binding to HMGR, the *C* value was 170, indicating experimental conditions were correct for accurate affinity determination.

To confirm that **1** competed with substrate, a binding experiment of **1** to HMGR was performed in the presence of 0.34 mM substrate, HMG-CoA. Figure 2b shows the binding isotherm obtained for the interaction of **1** with HMGR plus 0.34 mM HMG-CoA. A dramatic decrease in the slope of the binding curve indicated the apparent binding affinity of **1** to HMGR was reduced by excess substrate. This was as expected for a substrate competitive interaction. To determine actual binding affinity of **1** competing with substrate, the affinity of substrate needed to be factored into the equation to fit the experimental data. These equations have previously been developed by Sigurskjold and incorporated into Origin software developed by Microcal.[27] Parameters for the interaction of HMG-CoA with HMGR entered prior to fitting the experimental data were stoichiometry ($N = 1$), K_a (6.9×10^4 M^{-1}), ΔH (−9.0 kcal/M), and concentration of substrate (0.34 mM). Using the competition equation and thermodynamic parameters for HMG-CoA binding in parentheses, thermodynamic parameters for the binding interaction of **1** with HMGR in competition with HMG-CoA were $N = 0.92$, ΔH of –15.4 kcal/M, and K_d of 41 nM. Table 2 summarizes thermodynamic parameters for inhibitor **1** binding interactions with HMGR at 28 °C ± HMG-CoA. In Table 2, the difference in binding enthalpy of **1** plus or minus HMG-CoA was greater than 0.5 kcal/M, but this was reflective of the additive errors involved. In competition experiments, the measurement error for the binding enthalpy of HMG-Co to HMGR was added onto the measurement error for the binding enthalpy of **1** to HMGR containing HMG-CoA.

Heat capacity for the binding interaction of **1** to HMGR was determined by measuring ΔH for the interaction of **1** with HMGR in triplicate at four different temperatures. Results from the temperature dependence experiment are shown in Table 3.

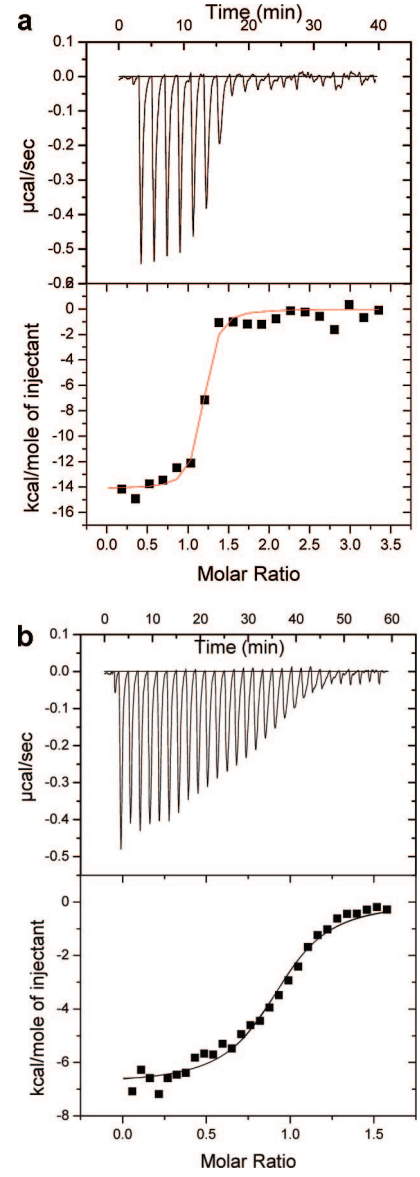

Figure 2. (a) Binding isotherm obtained by ITC using one 1 μL injection and nineteen 8 μL injections of 150 μM statin **1** into 10 μM HMGR at 28 °C in 10 mM Hepes, pH 7.2, 10% glycerol, 1 mM EDTA, 150 mM NaCl, 1.0 mM TCEP. (b) Binding isotherm obtained by ITC using one injection of 1 μL followed by twenty-nine 8 μL injections of 300 μM statin **1** into 340 μM HMG-CoA plus 8 μM HMGR at 28 °C in 10 mM Hepes, pH 7.2, 10% glycerol, 1 mM EDTA, 150 mM NaCl, and 1.0 mM TCEP.

Table 2. Thermodynamic Parameters for Statin **1** Binding Interactions with HMG-CoA Reductase and Statin **1** binding to HMG-CoA Reductase + 0.34 mM HMG-CoA at 28°C

ligand	K_a (M^{-1})	ΔG (kcal/M)	ΔH (kcal/M)	$-T\Delta S$ (kcal/M)
statin **1**	3.4×10^{7a}	-10.4 ± 0.4	-14.1 ± 0.4	3.7
statin **1** + 0.34 mM HMG-CoA	2.4×10^{7b}	-10.2 ± 0.2	-15.4 ± 0.1	5.2

[a] Determined using a single binding site model as described in the Experimental Section. [b] Determined using a competitive binding model with a stoichiometry of 1.0, K_a of 6.9e04 M^{-1}, and ΔH of –9.0 kcal/M for HMGCo-A binding to HMGR.

There was a temperature dependent change in binding enthalpy for the interaction with a heat capacity of –0.63 kcal/K^{-1} M^{-1} based on the slope of the plot of temperature versus change in binding enthalpy. This indicated there was a significant com-

Table 3. Temperature Dependence (Heat Capacity) of Statin **1** Interaction with HMGR by ITC

T (C)	*T* (K)	ΔH (kcal/M)[a]
28	301	−14.1
30	303	−17.9
35	308	−21.8
40	313	−25.3

[a] Average of three determinations.

Table 4. Results from the Measurement of Binding Enthalpy for Inhibitor **6** Interaction with HMGR in Buffers with Different Deprotonation Enthalpies at 30 °C

	ΔH deprotonation (kcal/M)	trial 1 ΔH (kcal/M)	trial 2 ΔH (kcal/M)	av ΔH (kcal/M)	ΔH std deviation (kcal/M)
Pipes	2.72	−8	−8.4	−8.2	0.3
Mes	3.7	−7.8	−7.9	−7.9	0.1
Hepes	4.99	−8.6	−9.1	−8.9	0.4
Bes	6.02	−8	−9.2	−8.6	0.8

ponent of binding energy due to hydrophobic interactions that increase with increasing temperature. The change in heat capacity was greater than for other marketed statins reported by Carbonell et al.[21]

Buffers with different enthalpies of ionization can also affect the binding enthalpies measured by ITC. To investigate the dependence on buffer conditions, the binding of **6** to HMGR was examined in four buffers with different enthalpies of ionization. Table 4 provides the binding enthalpies measured for statin **6** in each of the buffers. A linear regression of the data in Table 4 resulted in the following equation:

$$y = -0.21x - 7.5 \quad (1)$$

The slope of –0.21 was close to zero and indicated only negligible buffer effect (within experimental error) for the interaction. Lack of a coupled protonation−deprotonation reaction was previously reported for rosuvastatin.[21]

Structural Data Combined with Thermodynamic Parameters for Statin Inhibitors from the Imidazole Series Binding to HMGR. A high resolution crystal structure of **1** with HMGR was obtained and provided additional information to explain the increased binding enthalpy of **1** relative to other statins. Figure 3a shows the costructure of **1** bound to HMGR with a Connolly binding site surface shown. The binding surface was shaded according to hydrophobicity, with brown areas more hydrophobic, blue areas more hydrophilic, and green areas intermediate. There is a hydrophobic floor under the pyrrole extending under the *p*-fluorobenzyl substituent. The hydroxyl and carboxyl groups from the dihydroxyheptanoic acid substituent extend into hydrophilic pockets and form extensive H-bond networks with Glu559, Asn755, Lys691, Asp690, Arg590, Ser684, Lys692, and Lys735 (see Figure 3b). Because HMGR is tetrameric, ligand was bound in four different catalytic sites, permitting redundant analysis of the structure for deviations in positioning of the atoms. Table 5 lists the bond lengths for each H-bond that inhibitor **1** formed with HMGR for each of the four costructures of **1** bound to HMGR. Atom positioning of the ligand was very consistent for each of the four structures, as indicated by the consistency in the H-bond lengths. For the first member from each of the other series of templates in Table 1, H-bond lengths to the dihydroxyheptanoic acid substituent were nearly identical to those listed in Table 5, showing that the dihydroxyheptanoic acid interaction was highly conserved in each template series. This excludes the carboxyamide H-bond for **1** that was not always present in the other series or varied in position and length.

The carboxyamide of **1** forms a 2.6 Å H-bond of the amide carbonyl with Ser565 similar to that detected in atorvastatin.[18] Compared to atorvastatin, statin **1** has a methylene between the amide nitrogen and the phenyl group that permits flexing of the amide for optimal H-bonding partially reflected in greater binding enthalpy for **1** compared to **13**, a close analogue of atorvastatin. Greater binding enthalpy and retained high HMGR affinity of **1** suggests that the extra phenyl group and *ortho*-hydroxyl of **13** compared to **1** did not effectively contribute to binding affinity.

Hepatoselectivity of **1** was good, as indicated by the ratio of the IC_{50} for cholesterol inhibition in myocytes vs hepatocytes (Table 1, column L6/HEP); larger values for L6/HEP indicate greater hepatoselectivity. Greater binding enthalpy occurs with greater polar interactions and, as previously shown, greater polarity and hydrophilicity of the molecule is expected to provide improved active transport in hepatocytes.[9,14] Inhibitor **1** also showed modest in vivo activity (45% inhibition) in the mouse model, measuring inhibition of cholesterol synthesis (Table 1, MAICS, mouse acute inhibition of cholesterol synthesis).

Because the binding enthalpy of **1** was very good relative to other tight binding statins, some binding enthalpy could be sacrificed to gain binding free energy by adding hydrophobic substituents that are more optimally positioned than the phenyl group in **13**. Increasing the hydrophobic character of the fluorophenyl by adding another fluorine as exemplified in **2**, or by adding a biphenyl, **3**, slightly increased binding free energy and inhibition of cholesterol synthesis in the rat microsomal cholesterol synthesis assay (Table 1, RM IC_{50} = 0.3 and 3.6 nM, respectively) relative to **1**. Significantly increasing hyrophobicity as for **6** ($c \log D = 1.42$) with the *ortho*-fluorobiphenyl substituent provided one of the first inhibitors with subnanomolar activity (RM IC_{50}= 0.6 nM). But the structural alterations and increased hydrophobicity led to decreased hepatoselectivity. Binding enthalpy of **6** was 8.8 kcal/M less than **1**, but it gained 8.4 kcal/M in entropy therefore maintaining the same binding free energy.

Addition of an hydroxyethyl to the benzyl carbon, **4**, did not improve binding affinity. Consistent with this, analysis of the costructure for **4** indicated the hydroxyethyl was solvent exposed and did not form an H-bond with any HMGR residues. Inhibitor **4** maintained heptoselectivity but had less in vivo activity (18% inhibition) than **1**. Inhibitor **5** ($c \log D = -1.23$) was more polar than **1** ($c \log D = -0.84$), maintained affinity, hepatoselectivity, and inhibited cholesterol synthesis in vivo better than **1**. Results for inhibitors **1**–**6** indicated that while better affinity could be achieved through the addition of hydrophobicity to **1**, it came at the cost of hepatoselectivity. A better approach was to make structural alterations that increased hydrophilicity while maintaining binding enthalpy.

Inhibitors **7** and **8** had similar binding thermodynamic parameters as **1**, which was structurally similar to both but isomeric in positioning of substituents on the imidazole heterocycle. This suggested that the positioning of the nitrogen atoms on the imidazole heterocycle was not critical because it did not significantly alter binding affinity. Therefore even though the nitrogens of the imidazole heterocycle are H-bond acceptors, they were not participating in H-bonds to the protein backbone. This was confirmed by the costructures of **7** and **8**. Figure 4 shows the costructure of **7** bound to HMGR. The view of the binding site is oriented the same in Figures 3 and 4. Comparison of costructures show the substituents were positioned the same in the binding pockets for **1** and **7**. For **7**, the length of each

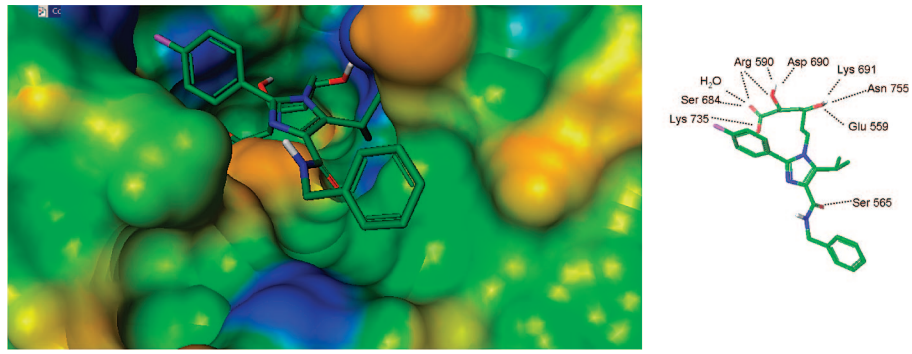

Figure 3. (left panel) Costructure of **1** (imidazole series) bound to HMGR. Inhibitor is colored by atom: carbon, green; nitrogen, blue; oxygen, red; hydrogen, white (not all hydrogens shown); fluorine, purple. Binding pocket is shown as a Connolly surface color coded by hydrophobicity: brown, more hydrophobic; green, intermediate; blue, hydrophilic. (right panel). Costructure of **1** bound to HMGR rotated so the benzyl group is down compared to left panel, showing hydrogen bonding to HMGR residues, see Table 5, column 3, for H-bond distances.

Table 5. H-Bond Lengths for Each of the Four Costructures of Inhibitor **1** Bound to Tetrameric HMGR

		costructure of inhibitor **1** binding to HMGR H-bond lengths (Å)			
inhibitor substituent	residue	molecule 1	molecule 2	molecule 3	molecule 4
carboxyamide	Ser565	2.6	2.5	2.5	2.6
DHHA OH[a]	Glu559	2.6	2.8	2.6	2.6
	Asn755	3.0		3.1	3.2
	Lys691	2.9	3.1	3.0	3.0
DHHA OH[b]	Asp690	2.7	2.8	2.7	2.5
	Arg590	3.2	3.1	3.2	3.3
	Arg590	3.1		2.9	
DHHA OH[c], C=O[c]	Arg590	3.4		3.5	
	H_2O	2.6	2.6	2.5	2.7
	Ser684	2.7	2.6	2.6	2.6
	Lys692	3.0	3.3	3.3	3.0
	Lys735	2.7	2.8	3.0	2.8

[a] H-bonds to the 3-OH of DHHA. [b] H-bonds of the 5-hydroxy of DHHA. [c] H-bonds to the carboxyl group of DHHA.

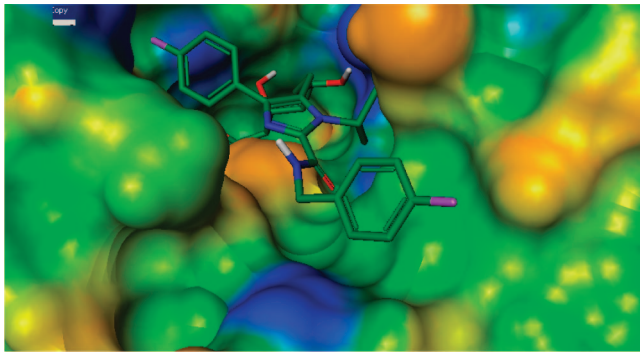

Figure 4. Costructure of **7** bound to HMGR. Inhibitor and binding pocket color is coded as in Figure 3. HMGR is in the same orientation as Figure 3.

H-bond to the DHHA and carboxyamide substituents was within 0.3 Å of those for **1** listed in Table 5. While **7** and **8** showed good in vivo activity (49% and 74% inhibition, respectively), they were not as hepatoselective as **1** or **5**.

Structural Data Combined with Thermodynamic Parameters for Statin Inhibitors from the Bicyclic Pyrrole Series Binding to HMGR. While bicyclic pyrroles have lower binding enthalpy than **1**, they each showed favorable binding entropy contributing to binding free energy, ΔG. The increased entropic

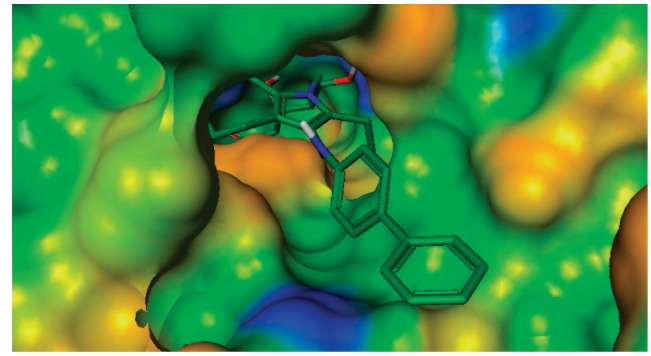

Figure 5. Costructure of **9** bound to HMGR. Inhibitor **9** is from the bicyclic pyrrole series and produces ordering of the C-terminal region of HMGR similar to that detected in complexes with substrate. Ordering of the C-terminal residues is referred to in this work as the flap closed conformation. Inhibitor and binding pocket color is coded as in Figure 3. HMGR is in the same orientation as Figure 3.

binding component resulted in a ΔG of HMGR binding for **9** that was the same as that measured for **1**. Favorable binding entropies of these inhibitors were evident from examination of the high resolution crystal structures for the cocomplexes. The costructure for **9** cocomplexed to HMGR is shown in Figure 5. HMGR was positioned in the same orientation for Figures 3–5. The bicyclic ring system displaces ordered water molecules from the active site but also ordered the C-terminal residues Gly860 to Ser865 that are normally disordered in statin inhibitor bound structures. This flap folds over the catalytic site, forming hydrophobic interactions with the bicyclic portion of the inhibitor. In the view of the costructure for **9**, not all of the seven-membered ring or the DHHA moiety is seen because the flap partially covers the opening to the catalytic site. Most of the pyrrole, carboxyamide, and biphenyl ring are seen. Figure 6 shows a comparison of **1** (Figure 6a) and **9** (Figure 6b) using a ribbon diagram for depiction of the HMGR backbone. In this view, it is easier to see the C-terminal residues. Electron density for the C-terminal residues past Gly860 were not detected in the costructure of **1** bound to HMGR and the residues are not shown. There was electron density for these residue in the costructure of **9** with HMGR and the residues are shown, making van der Waal's contact with the inhibitor. Ordering of the C-terminal flap is similar to what is found in substrate−complex structures.[18]

It is not intuitive that ordering the flap would produce favorable binding entropy, but displacement of several ordered water molecules from the catalytic site and from the solvent shell around the ligand due to hydrophobic interactions with

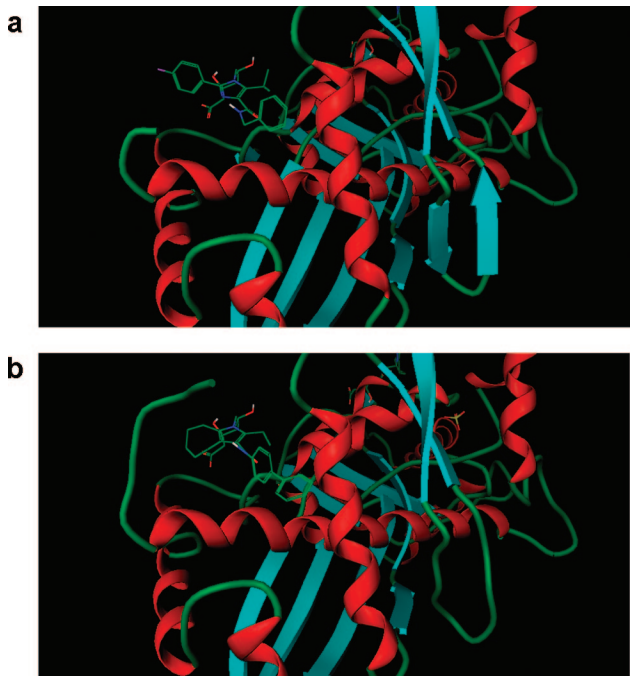

Figure 6. (a) Statin **1** bound to HMGR. Electron density for the C-terminal residues 861–865 was not apparent in the costructure and is not shown. Inhibitor color coding is the same as in Figure 3. Protein is depicted in a ribbon diagram colored by secondary structural feature: α helix, red; β sheet, cyan; unordered, green. (b) Statin **9** bound to HMGR. Electron density for the C-terminal residues (His861, Leu862, Val863, Lys864, Ser865) was detected in the costructure, and this conformation is referred to as the flap closed conformation. Inhibitor color coding is the same as in Figure 3. Protein is depicted in a ribbon diagram colored by secondary structural feature: α helix, red; β sheet, cyan; unordered, green.

HMGR would contribute to the favorable binding entropy. Interestingly, examination of the costructures indicated this flap is closed for each of the bicyclic inhibitors (**9**–**12**) of series 4. Therefore, it appears to be a general property of this series of inhibitors and probably occurs due to unique hydrophobic interactions with the hydrophobic bicyclic moiety. It also suggests that transposing the hydrophobic bicyclic nature into the imidazole template could combine favorable binding enthalpy of the imidazole series with favorable binding entropy of the bicyclic series, potentially resulting in even greater binding free energy.

Inhibitor **12** showed reasonable hepatoselectivity (L6/HEP = 1487), but it showed only weak in vivo activity (MAICS = 23%). While inhibition in rat muscle myocytes was not tested for **9**–**11**, they also showed only weak in vivo activity in the MAICS assay.

Structural Data Combined with Thermodynamic Parameters for Statin Inhibitors from the Pyrrole Series Binding to HMGR. Although there are more structural differences than the substitution pattern on the pyrrole heterocycle, comparison of thermodynamic parameters for **13** and **20** indicated that the position of the nitrogen in the pyrrole ring did not have a large influence on binding affinity. In addition to the isomeric position of the substituents, differences in the two structures were **13** had an *ortho*-phenoxy and **20** had a *para*-fluoro substituent. Figure 7 shows the costructures of **13** and **20** bound to HMGR. For comparison, all atoms for **20** were colored cyan. Costructures indicated the pyrrole subsituents were positioned in the binding pocket in the same orientation whether the DHHA was on the pyrrole nitrogen or the α carbon. Rotation of the *ortho*-phenoxy of **13** was evident relative to the unsubstituted carboxybenzamide of **20**. A weak polar interaction of the phenoxy with HMGR could favor positioning of the ring in this conformation relative to **20**.

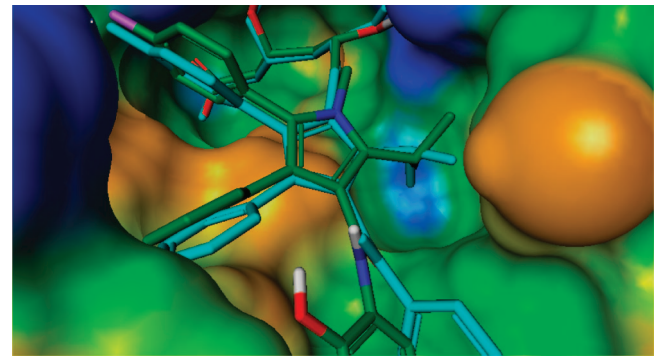

Figure 7. Costructure of **13** bound to HMGR overlaid with the costructure of **20** bound to HMGR. Inhibitor **13** and binding pocket colors are coded as in Figure 3. For better contrast, all atoms for **20** are shown in cyan. Binding site is rotated compared to orientation in Figure 3–5.

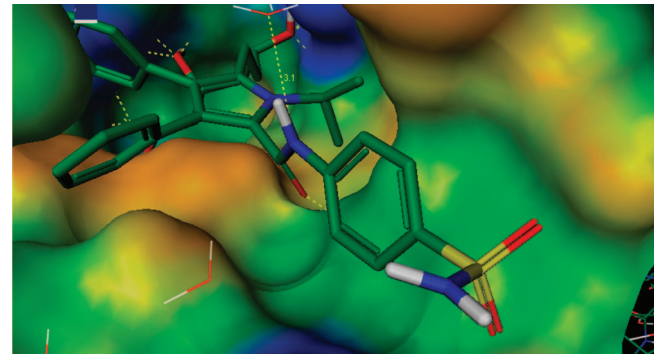

Figure 8. Costructure of **15** bound to HMGR. Except for the sulfur atom colored yellow, inhibitor and binding pocket color is coded as in Figure 3. Yellow dashed lines are representative of H-bonds, and water molecules are depicted.

Inhibitor **13** had an increased HMGR binding affinity $\Delta\Delta G$ (0.6 kcal/M) and $\Delta\Delta H$ (1.4 kcal/M) relative to **14**, the other atorvastatin analogue. The polar interaction of the phenoxy would be expected to contribute favorably to the binding enthalpy. Binding entropy was less favorable for **13** relative to **14**, suggesting that the 3-phenyl substituent on the pyrrole, which is partially solvent exposed, did not contribute significantly more binding free energy than the isopropyl substituent.

The costructure of **15** (Figure 8) with HMGR showed the same H-bonding pattern of the DHHA substituent as detected for **13**. In addition, the benzamide C═O formed an H-bond with Ser565, and for **15**, the benzamide amine H-bonded to a water molecule. Although the *p*-sulfonamide did not form H-bonds with HMGR, the backbone amide nitrogen of Ser565 was 4.5 Å away. This and other polar functionality of HMGR could form weak polar interactions to the *p*-sulfonamide substituent of **15**. The amine portion of the sulfonamide was largely solvent exposed. With the solvent exposure, less desolvation penalty was paid for burying the *p*-sulfonamide, but the weak polar interactions produced no significant increase in affinity from the sulfonamide substituent. Inhibitor **15** had good hepatoselectivity (L6/HEP = 6704) and some in vivo efficacy (MAICS = 32% inhibition).

Binding free energies were within 1.3 kcal/M for inhibitors **15**–**22** and, except for **19** and **22**, inhibition in the rat microsomal

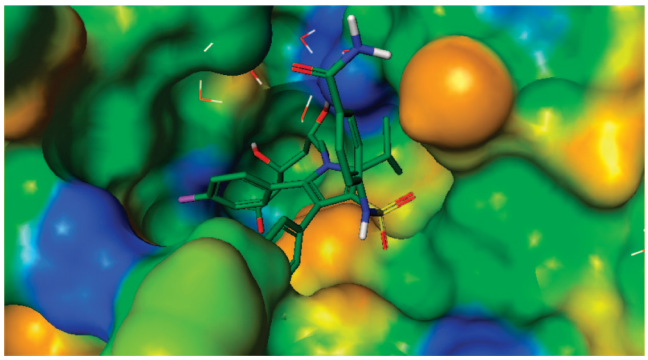

Figure 9. Costructure of **23** bound to HMGR. Except for the sulfur atom colored yellow, inhibitor and binding pocket color is coded as in Figure 3. Water molecules are depicted.

cholesterol synthesis assay were similar, spanning a range from 1.3 to 3.0 nM. There were larger differences in binding enthalpies for the set, with the most hydrophilic inhibitors **15**–**17** having the greatest binding enthalpies between 13.1 and 13.7 kcal/M. These binding enthalpies were at least 0.9 kcal/M greater than binding enthalpies for **18**–**22**. Excluding **22**, there was a linear relation between binding enthalpy (ΔH) and calculated hydrophillicity (*c* log *D*) with a correlation coefficient of 0.74, but significant structural changes such as found in the bicyclic inhibitor **22** resulted in an outlier. A favorable ΔS of 2.7 kcal/M for the binding interaction of **22** with HMGR was unique compared to **15**–**21**. Favorable entropy and the bicyclic structure of this analogue were also characteristic of the bicyclic pyroles, series 3. Indeed, the costructure of **22** with HMGR indicated the protein was in the flap closed conformation, similar to that detected for the bicyclic pyroles (see Protein Data bank file 2Q6B).

Although ΔH was equivalent for inhibitors **15** and **16**, within experimental error, binding affinity of **16** to HMGR was slightly greater than for **15**, ~4 fold. The crystal structure and lack of difference compared to the phenyl substituent found in **16**, suggested that interactions of the sulfonamide from **15** to HMGR did not contribute significantly to binding free energy. Inhibitor **16** with fewer rotatable bonds paid less entropic penalty than **15** and with lower molecular weight was more ligand efficient.[28] Inhibitor **16** also had better in vivo activity (MAICS = 53% inhibition). All binding thermodynamic parameters for **17** were within 0.5 kcal/M to those of **16**, suggesting the *p*-dimethyl formamide R2 substituent of **17** also did not form a productive H-bond with protein. Inhibitor **17** (L6/HEP = 271) was less hepatoselective than **15** with better in vivo activity (MAICS = 59% inhibition).

Thermodynamic parameters for the interactions of inhibitors **19**–**21** with HMGR were within 1.0 kcal/M. Cholesterol inhibition in rat hepatocytes was similar for **20** and **21**, HEP IC_{50} = 1.03 and 2.81 nM, respectively, indicating the fluorine substituent on R1 did not improve affinity or potency for the series. The amidopyrrole **19** with a *p*-methyl ester R2 substituent had the best cholesterol inhibition in rat hepatocytes at 0.12 nM, had good in vivo activity (MAICS = 64%), but was less hepatoselective than imidazole inhibitors from series 1.

Inhibitors **23**–**25** from pyrrole series 6 had equivalent ΔH of binding. There were relatively small differences in ΔS, resulting in marginal changes in affinity. Again, they have similar structures except for the sulfonamide substituents, suggesting that the sulfonamide substituents are not contributing significantly to the binding free energy. This was reflected in the costructures for the inhibitors. Figure 9 shows the binding interaction of **23** with HMGR. The sulfonamide did not form an H-bond with Ser565 and the *p*-phenylamide portion was highly solvent exposed consistent with the thermodynamic finding that substituents off the sulfonamide had little effect on binding free energy. Inhibition of cholesterol synthesis in rat hepatocytes was also similar for **23**–**25** and ranged from 0.8 to 1.8 nM.

Conclusions

As part of a discovery program to identify potent and hepatoselectivity statins, thermodynamic binding data were used to aid in template prioritization and analogue design. Because entropically driven ligand−protein binding is typically associated with hydrophobic interactions, whereas enthalpically driven binding is driven through electrostatic and H-bonding interactions, templates with greater enthalpic components to their binding interactions were selected as a way to minimize inhibitor lipophilicity and increase hepatoselectivity. Utilizing this approach in combination with structure–activity studies, inhibitor **1** was selected for further evaluation based on its excellent HMGR affinity, binding enthalpy, biological potency, and hepatoselectivity.

Experimental Section

Protein Expression, Purification, and Crystallization. The structure of HMG-CoA reductase (HMGR) in complex with statins has previously been reported.[18] A modified version of the published clone was used for this study. HMGR was expressed as an N-terminal His6 protein truncated from amino acid 441–875 with the mutation M485I in the *Escherichia coli* strain BL21 STAR. Protein was purified via Ni-affinity and gel filtration chromatography. HMGR was concentrated to 20 mg/mL and then complexed with statins at a concentration of 0.5 mM and incubated at 4 °C for 1 h. Crystals were prepared in hanging drops from a crystallization solution of 28% PEG 4000, 0.1 mM Tris, pH 8.5, 0.2 M Li_2SO_4, and 50 mM DTT at 20 °C. Diffraction quality crystals (P21) were obtained after microseeding, harvested after 1 week, and cryoprotected in 25% ethylene glycol. Data were collected at 2 Å resolution at the Industrial Macromolecular Crystallography Association Collaborative Access Team beam-line ID-17 at the Advanced Photon Source (Argonne National Laboratory). All data were processed and scaled using HKL2000. Costructures for inhibitors bound to HMGR that are provided in the figures are deposited in the Protein Data Bank (see Supporting Information for accession file names). Three-dimensional molecular visualization and drug design (MoVit, version 2.12) software, developed at Pfizer, was used to display and plot crystallographic data shown in this work.

HMGR Inhibitors, HMG-CoA, and Buffer Reagents. All HMGR inhibitors reported in this work were synthesized at Pfizer, Inc.[10–13,29,30] HMG-CoA and all buffer reagents were purchased from Sigma-Aldrich Chemical company.

Isothermal Titration Calorimetry. Isothermal titration calorimetry (ITC) experiments were performed using an Microcal VP ITC and a Microcal automated VP-ITC. Data collection, analysis, and plotting were performed using a Windows-based software package (Origin, version 7.0) supplied by Microcal. The titrating microcalorimeter consisted of a sample and reference cell held in an adiabatic enclosure. To minimize heat of dilution effects resulting from differences in buffer composition between ligand and protein, ligands were dissolved in dialysate buffer from the final step in the HMGR purification. Dialysate buffer was 10 mM Hepes, pH 7.2, 10% glycerol, 1 mM EDTA, 150 mM NaCl, and 1.0 mM TCEP. Ligand and protein solutions were degassed prior to analysis. The concentration of HMGR was determined spectroscopically by measuring A_{280} and A_{260} and using the following:

$$[\text{HMGR}]\text{mg/mL} = (A_{280} \times 1.55) - (A_{280} \times 0.76)/0.594 \quad (2)$$

The molecular weight of monomeric HMGR was 47.5 kDa and for the catalytic tetramer 190 kDa. Typically, a preliminary injection of 1 μL followed by 19 injections of 8 μL of inhibitor solution at 100−150 μM were made by a computer controlled injector into

the sample cell filled with 1.37 mL of HMGR solution at 20–80 μM based on monomer. The syringe stir rate was 300 rpm. Heat adsorbed or released with each injection was measured by the calorimeter. Titration isotherms for the binding interactions were composed of the differential heat flow for each injection. These were integrated to provide the enthalpy change with each injection. Heats of dilution obtained by injecting HMGR into final purification buffer were insignificant. Isotherms fit well to a single-site model using an iterative nonlinear least-squares algorithm.[26] All parameters were floated during the iterations. Binding isotherms fit by this method provided the equilibrium association or binding constant, K_a, the change in enthalpy, ΔH, and stoichiometry of binding, N. Binding stoichiometry was adjusted to 1:1 when necessary (four molecules of ligand per tetrameric HMGR). The change in free energy (ΔG) and change in entropy (ΔS) were then determined using the following equation:

$$\Delta G = -RT \ln K_a = \Delta H - T\Delta S \quad (3)$$

where R is the universal gas constant, T is the temperature in degrees Kelvin, and other parameters are as previously defined.

Some statins bound with high affinities, and experiments for these were also conducted with substrate added to HMGR prior to titration with ligand. These experiments permitted more accurate determination of the inhibitor affinity and confirmation that the inhibitor was competitive with substrate. Competition experiments like these have previously been utilized to study binding of other enzyme systems.[27] Binding isotherms from the current competition studies were fit using competitive binding equations previously developed by Sigurskjold and implemented in Microcal Origin software.

In addition, experiments were conducted in several buffers of different hydrogen ionization potential to determine the role of protons in the binding interaction.[31] For these experiments, HMGR was 2× dialyzed versus buffer, 0.2 μM filtered, and then ligands were dissolved in dialysate buffer.

Acknowledgment. The authors thank Dr. Barry Finzel for preparing the crystallographic files for submission to the Protein Data bank.

Supporting Information Available: Cocomplex structures for the compounds are available in the Protein Data Bank. This material is available free of charge via the Internet at http://pubs.acs.org.

References

(1) Rosamond, W.; Flegal, K.; Friday, G.; Furie, K.; Go, A.; Greenlund, K.; Haase, N.; Ho, M.; Howard, V.; Kissela, B.; Kittner, S.; Lloyd-Jones, D.; McDermott, M.; Meigs, J.; Moy, C.; Nichol, G.; O'Donnell, C. J.; Roger, V.; Rumsfeld, J.; Sorlie, P.; Steinberger, J.; Thom, T.; Wasserthiel-Smoller, S.; Hong, Y. Heart Disease and Stroke Statistics—2007 Update: A Report From the American Heart Association Statistics Committee and Stroke Statistics Subcommittee. *Circulation* **2007**, *115*, e69–e171.

(2) Poulter, N. R. Past, present, and future clinical trials of cardiovascular risk reduction: The hyperlipidemia perspective. *Int. Congr. Ser.* **2004**, *1262*, 265–268.

(3) Stein, E. A. Management of dyslipidemia in the high-risk patient. *Am. Heart J.* **2002**, *144*, S43–S50.

(4) Blumenthal, R. S. Statins: Effective antiatherosclerotic therapy. *Am. Heart J.* **2000**, *139*, 577–583.

(5) Smith, S. C. Review of Recent Clinical Trials of Lipid Lowering in Coronary Artery Disease. *Am. J. Cardiol.* **1997**, *80*, 10H–13H.

(6) Mason, R. P.; Walter, M. F.; Day, C. A.; Jacob, R. F. Intermolecular Differences of 3-Hydroxy-3-Methylglutaryl Coenzyme A Reductase Inhibitors Contribute to Distinct Pharmacologic and Pleiotropic Actions. *Am. J. Cardiol.* **2005**, *96*, 11–23.

(7) Baer, A. N.; Wortmann, R. L. Myotoxicity associated with lipid-lowering drugs. *Curr. Opin. Rheumatol.* **2007**, *19*, 67–73.

(8) Bruckert, E.; Hayem, G.; Dejager, S.; Yau, C.; Begaud, B. Mild to Moderate Muscular Symptoms with High-Dosage Statin Therapy in Hyperlipidemic Patients: The PRIMO Study. *Cardiovasc. Drugs Ther.* **2006**, *19*, 403–414.

(9) Rosenson, R. S. Current overview of statin induced myopathy. *ACC Curr. J. Rev.* **2004**, *13*, 11–12.

(10) Bratton, L. D.; Auerbach, B.; Choi, C.; Dillon, L.; Hanselman, J. C.; Larsen, S. D.; Lu, G.; Olsen, K.; Pfefferkorn, J. A.; Robertson, A.; Sekerke, C.; Trivedi, B. K.; Unangst, P. C. Discovery of pyrrole-based hepatoselective ligands as potent inhibitors of HMG-CoA reductase. *Bioorg. Med. Chem.* **2007**, *15*, 5576–5589.

(11) Larsen, S. D.; Poel, T.-J.; Filipski, K. J.; Kohrt, J. T.; Pfefferkorn, J. A.; Sorenson, R. J.; Tait, B. D.; Askew, V.; Dillon, L.; Hanselman, J. C.; Lu, G. H.; Robertson, A.; Sekerke, C.; Kowala, M. C.; Auerbach, B. J. Pyrazole inhibitors of HMG-CoA reductase: An attempt to dramatically reduce synthetic complexity through minimal analog redesign. *Bioorg. Med. Chem. Lett.* **2007**, *17*, 5567–5572.

(12) Pfefferkorn, J. A.; Choi, C.; Song, Y.; Trivedi, B. K.; Larsen, S. D.; Askew, V.; Dillon, L.; Hanselman, J. C.; Lin, Z.; Lu, G.; Robertson, A.; Sekerke, C.; Auerbach, B.; Pavlovsky, A.; Harris, M. S.; Bainbridge, G.; Caspers, N. Design and synthesis of novel, conformationally restricted HMG-CoA reductase inhibitors. *Bioorg. Med. Chem. Lett.* **2007**, *17*, 4531–4537.

(13) Pfefferkorn, J. A.; Song, Y.; Sun, K.-L.; Miller, S. R.; Trivedi, B. K.; Choi, C.; Sorenson, R. J.; Bratton, L. D.; Unangst, P. C.; Larsen, S. D.; Poel, T.-J.; Cheng, X.-M.; Lee, C.; Erasga, N.; Auerbach, B.; Askew, V.; Dillon, L.; Hanselman, J. C.; Lin, Z.; Lu, G.; Robertson, A.; Olsen, K.; Mertz, T.; Sekerke, C.; Pavlovsky, A.; Harris, M. S.; Bainbridge, G.; Caspers, N.; Chen, H.; Eberstadt, M. Design and synthesis of hepatoselective, pyrrole-based HMG-CoA reductase inhibitors. *Bioorg. Med. Chem. Lett.* **2007**, *17*, 4538–4544.

(14) Hamelin, B. A.; Turgeon, J. Hydrophilicity/lipophilicity: relevance for the pharmacology and clinical effects of HMG-CoA reductase inhibitors. *Trends Pharmacol. Sci.* **1998**, *19*, 26–37.

(15) Istvan, E. S. Bacterial and mammalian HMG-CoA reductases: related enzymes with distinct architectures. *Curr. Opin. Struct. Biol.* **2001**, *11*, 746–751.

(16) Istvan, E. S. Structural mechanism for statin inhibition of 3-hydroxy-3-methylglutaryl coenzyme A reductase. *Am. Heart J.* **2002**, *144*, S27–S32.

(17) Istvan, E. S.; Deisenhofer, J. The structure of the catalytic portion of human HMG-CoA reductase. *Biochim. Biophys. Acta* **2000**, *1529*, 9–18.

(18) Istvan, E. S.; Deisenhofer, J. Structural Mechanism for Statin Inhibition of HMG-CoA Reductase. *Science* **2001**, *292*, 1160–1164.

(19) Tabernero, L.; Rodwell, V. W.; Stauffacher, C. V. Crystal Structure of a Statin Bound to a Class II Hydroxymethylglutaryl-CoA Reductase. *J. Biol. Chem.* **2003**, *278*, 19933–19938.

(20) Endo, A.; Kuroda, M.; Tanzawa, K. Competitive inhibition of 3-hydroxy-3-methylglutaryl coenzyme a reductase by ML-236A and ML-236B fungal metabolites, having hypocholesterolemic activity. *FEBS Lett.* **1976**, *72*, 323–326.

(21) Carbonell, T.; Freire, E. Binding Thermodynamics of Statins to HMG-CoA Reductase. *Biochemistry* **2005**, *44*, 11741–11748.

(22) Ong, K. K.; Khor, H. T.; Tan, D. T. S. Assay of 3-hydroxy-3-methylglutaryl CoA reductase activity using anionic-exchange column chromatography. *Anal. Biochem.* **1991**, *196*, 211–214.

(23) Ness, G. C.; Chambers, C. M.; Lopez, D. Atorvastatin action involves diminished recovery of hepatic HMG-CoA reductase activity. *J. Lipid Res.* **1998**, *39*, 75–84.

(24) Holdgate, G. A.; Ward, W. H. J.; McTaggart, F. Molecular mechanism for inhibition of 3-hydroxy-3-methylglutaryl CoA (HMG-CoA) reductase by rosuvastatin. *Biochem. Soc. Trans.* **2003**, *33*, 528–531.

(25) Lafont, V.; Armstrong, A. A.; Ohtaka, H.; Kiso, Y.; Mario Amzel, L.; Freire, E. Compensating Enthalpic and Entropic Changes Hinder Binding Affinity Optimization. *Chem. Biol. Drug Des.* **2007**, *69*, 413–422.

(26) Wiseman, T.; Williston, S.; Brandts, J. F.; Lin, L. N. Rapid measurement of binding constants and heats of binding using a new titration calorimeter. *Anal. Biochem.* **1989**, *179*, 131–137.

(27) Sigurskjold, B. W. Exact Analysis of Competition Ligand Binding by Displacement Isothermal Titration Calorimetry. *Anal. Biochem.* **2000**, *277*, 260–266.

(28) Hopkins, A. L.; Groom, C. R.; Alex, A. Ligand efficiency: a useful metric for lead selection. *Drug Discovery Today* **2004**, *9*, 430–431.

(29) Pfefferkorn, J. A.; Bowles, D. M.; Kissel, W.; Boyles, D. C.; Choi, C.; Larsen, S. D.; Song, Y.; Sun, K.-L.; Miller, S. R.; Trivedi, B. K. Development of a practical synthesis of novel, pyrrole-based HMG-CoA reductase inhibitors. *Tetrahedron* **2007**, *63*, 8124–8134.

(30) Watanabe, M.; Koike, H.; Ishiba, T.; Okada, T.; Seo, S.; Hirai, K. Synthesis and Biological Activity of Methanesulfonamide Pyrimidine- and *N*-Methanesulfonyl Pyrrole-Substituted 3,5-Dihydroxy-6-heptenoates, a Novel Series of HMG-CoA Reductase Inhibitors. *Bioorg. Med. Chem.* **1997**, *5*, 437–444.

(31) Doyle, M. L.; Louie, G.; Dal Monte, P. R.; Sokoloski, T. D. Tight binding affinities determined from thermodynamic linkage to protons by titration calorimetry. In *Energetics of Biological Macromolecules*; Methods in Enzymology, Vol. 259; Johnson, M. L., Ackers, G. K., Eds.; Academic Press: San Diego, 1995; pp 183–194.

JM7015057